SMASIS2014-7611

DESIGN AND VALIDATION OF ACCELERATION MEASUREMENT USING THE MARTLET WIRELESS SENSING SYSTEM

Xinjun Dong, Dapeng Zhu, Yang Wang
School of Civil and Environmental Engineering, Georgia Institute of Technology, Atlanta, GA 30332 USA

Jerome P. Lynch
Department of Civil and Environmental Engineering,
University of Michigan, Ann Arbor, MI 48109, USA

R. Andrew Swartz
Department of Civil and Environmental Engineering,
Michigan Technological University, Houghton, MI 49931, USA

ABSTRACT

The adoption of wireless sensing technology by the structural health monitoring community has shown advantages over traditional cable-based systems, such as convenient sensor installation and lower system cost in many applications. Recently, a new generation of wireless sensing platform, named Martlet, has been collaboratively developed by researchers at the University of Michigan, Georgia Tech, and Michigan Tech. Martlet adopts a Texas Instruments Piccolo microcontroller running up to 90 MHz clock frequency, which enables Martlet to support high-frequency data acquisition and high-speed onboard computation. The extensible design of the Martlet printed circuit boards allows convenient incorporation of various sensor boards. In order to obtain accurate acceleration data and meanwhile reduce the sensor cost, a new Martlet sensor board, named integrated accelerometer wing, is developed. The integrated accelerometer wing adopts a commercial-off-the-shelf MEMS (microelectromechanical systems) accelerometer and contains an onboard signal conditioner performing three basic functions, including mean shifting, anti-aliasing filtering and signal amplification. One distinct feature of the signal conditioner is the on-the-fly programmable cut-off frequency and amplification gain factor. To validate the performance of Martlet and the integrated accelerometer wing, experiments are carried out on a laboratory four-story aluminum shear-frame structure. The laboratory experiment results demonstrate that the performance of the wireless sensing system is comparable to that of cabled reference sensors. In addition, using data collected by wireless sensors, vibration modal properties of the structure are identified and finite element (FE) model updating is performed.

INTRODUCTION

Civil structures, including buildings, bridges, tunnels, etc., are complex engineering systems that exist in large quantities in modern society. Taking bridges for example, the United States has 607,751 bridges in operation in 2013 [1]. As bridges are continuously exposed to harsh outdoor environment and traffic loading, structural safety condition may deteriorate significantly throughout the designed service life. The latest ASCE 2013 report card shows that one in nine of the nation's bridges are rated as structurally deficient [2]. In order to facilitate the safety assessment of structures, structural health monitoring (SHM) systems have been widely studied for monitoring structural performance and identifying potential damage [3, 4]. Among various SHM approaches, vibration-based monitoring using accelerometers plays an important role. Important structural characteristics, such as modal properties, can be extracted based on the acceleration measurements [5, 6]. In addition, some studies propose to use measured acceleration responses for detecting structural defects [7, 8].

In order to obtain more detailed structural information, it is preferred to install a large amount of sensors on the structure. Traditional SHM systems adopt lengthy coaxial cables for transmitting data from structural sensors, which results in high installation cost and is labor intensive [9]. In order to overcome the limitation of cabled SHM systems, significant efforts have been devoted to developing wireless SHM systems [10, 11]. The performance of wireless SHM systems has been validated in laboratory and field experiments[12, 13]. Such a system can contain tens or hundreds of wireless sensing nodes, each node with its own set of sensors, signal digitizer, microprocessor, and wireless transceiver.

This paper reports the latest development of a low-cost wireless sensing node for SHM, named Martlet [14]. A Texas Instruments Piccolo microcontroller, running up to 90 MHz clock frequency, is adopted in Martlet to execute onboard computation and data acquisition. The dual-core architecture of the microcontroller enables parallel tasks to be simultaneously performed on the main core and a programmable control law accelerator (CLA) core. In addition, the 32-bit floating-point math accelerator on the CLA enables faster and more accurate onboard computation. An onboard Micro SD card reader provides additional memory for data storage. The power-amplified wireless transceiver on the Martlet node enables reliable communication up to 1,600 ft. The extensible design allows Martlet to easily incorporate various sensor boards, which are referred as Martlet wings. In order to reduce the sensor cost and meanwhile obtain accurate acceleration data, a Martlet sensor board, named integrated accelerometer wing, is recently developed. The accelerometer wing integrates a low-cost tri-axial MEMS (microelectromechanical system) accelerometer and associated signal conditioning circuit for low-cost acceleration measurement. The cut-off frequencies and amplification gains of the signal conditioning circuit can be programmed on the fly.

The performance of the wireless sensing system is validated through laboratory experiments. The integrated accelerometer wing is installed on a four-story aluminum shear-frame structure in the lab. The accuracy of the wireless acceleration measurement is evaluated with cabled accelerometers as reference. Furthermore, modal properties of the structure are extracted from the wireless acceleration measurement. Two finite element (FE) model updating approaches are applied for comparison, one minimizing modal dynamic residual and the other minimizing modal property difference between simulated and measurement results.

The rest of the paper is organized as follows. The development of Martlet node and integrated accelerometer wing is first introduced. The performance evaluation of wireless sensing system is then described. The modal analysis and model updating results are presented. Finally, a summary and discussion are provided.

DESIGN OF MARTLET WIRELESS SENSING NODE

This section describes the design and development of the Martlet wireless sensing node. The section first introduces overall design of the Martlet node. The development of the integrated accelerometer wing is then presented.

Martlet node

Martlet, as shown in Fig. 1, is a next-generation low-cost wireless sensing node developed for SHM applications [14]. The development of Martlet is a joint effort among the Laboratory for Intelligent Systems and Technologies at the University of Michigan, the Laboratory for Smart Structural Systems at Georgia Institute of Technology, and the Department of Civil and Environmental Engineering at Michigan

Technological University. The Martlet wireless node adopts a Texas Instruments Piccolo microcontroller as the core processor to execute onboard computation and data acquisition. The clock frequency of an earlier version (TMX320F28069) of the microcontroller can be programmed up to 80 MHz, and a more recent version (TMS320F28069) can support up to 90 MHz. The dimension of the Martlet node is 2.5 in by 2.25 in.

One distinct feature of the microcontroller is the capability of high-speed data acquisition. The direct memory access (DMA) module on the microcontroller allows the Martlet node to collect sensor data at a sampling rate up to 3 MHz. In addition, various general purpose input/output (GPIO) pins are extended to the wing connectors from the microcontroller, which allow communication between the Martlet motherboard and peripheral wing boards using protocols such as serial peripheral interface (SPI), inter-integrated circuit (I^2C), and pulse width modulation (PWM), etc. There is 100 kB × 16-bit random access memory (RAM) available in the microcontroller for embedded computing. To extend the data storage size of the Martlet node, a typical Micro SD card (like these used in digital cameras) can be plugged into the motherboard. The data stored in the Micro SD card can be either wirelessly transferred or easily read offline by a personal computer. The Martlet node adopts a 2.4 GHz radio for low-power wireless communication through IEEE 802.15.4 standard [15]. The communication range can reach up to 1,600 ft at line-of-sight, and the maximum transfer rate can reach 250 kbps. The extensible hardware design feature of the Martlet node enables various sensor boards to conveniently stack up through four wing connectors and work with the Martlet motherboard. The combination of the extensible design feature with onboard 9-channel 12-bit analog-
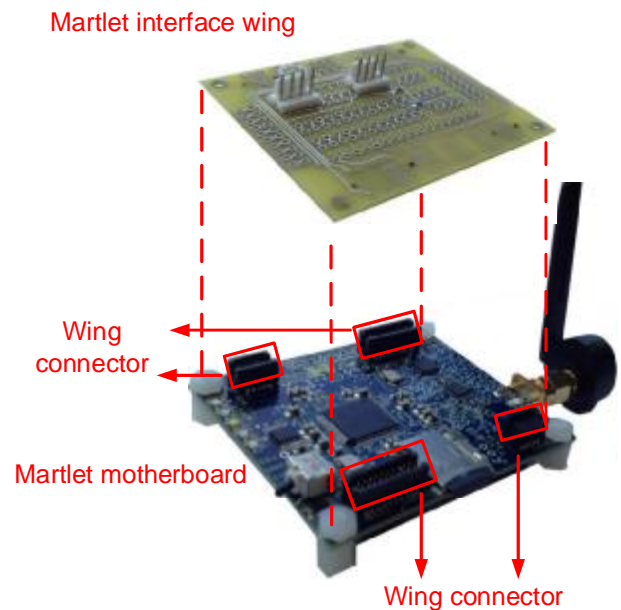

Fig. 1. The Martlet wireless node with wing connectors
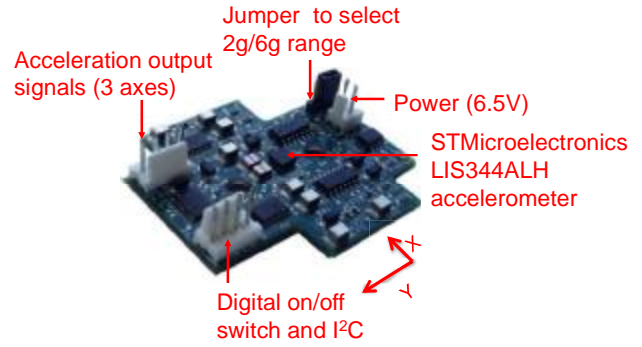(2.5 in × 2.25 in)

to-digital conversion (ADC) allows the Martlet node to simultaneously sample analog signals from multiple sensors through different accessory sensor boards (termed "wing" boards).

To this end, several wing boards have been developed for various applications, including ultrasonic sensing, strain measurement, fluid flow measurement, pump and valve control, CO_2 and temperature monitoring, motor control, and accurate time keeping with a real-time clock (RTC) [14]. A general ADC/DAC wing has also been developed to provide passband to generic analog sensor signals, with programmable cut-off frequency and amplification gains. The ADC/DAC wing also provides two analog output channels for real-time feedback applications such as structural control [16].

Integrated accelerometer wing

In order to obtain accurate acceleration measurement, and in the meantime reduce sensor cost, one solution is to integrate a low-cost MEMS accelerometer and specialized signal conditioning circuit into a single wing board, as shown in Fig. 2(a). The integrated accelerometer wing adopts a tri-axial MEMS accelerometer, the STMicroelectronics LIS344ALH model. A jumper on the board selects between ±2g and ±6g measurement scales. The noise density of the measurement is 25 $\mu g / \sqrt{Hz}$ along the x-axis and y-axis, and $50\,\mu g / \sqrt{Hz}$ along the z-axis.

The analog signals from the LIS344ALH accelerometer are directly fed into an onboard signal conditioner that performs mean shifting, low-pass filtering, and amplification (Fig. 3). The mean shifting module is particularly useful because the zero-g output voltage signals from the LIS344ALH accelerometer depend on the orientation of the accelerometer mount. Regardless of zero-g voltage levels of the sensor signals, the mean-shifted signals oscillate around 1.65V and the dynamic waveform remains the same as prior to shifting. Next, the anti-aliasing module prevents high-frequency signals and noises from irreversibly contaminating the digitalized data samples. A 4th-order low-pass Bessel filter with a programmable cutoff frequency is adopted in this anti-aliasing design. The phase shift of a Bessel filter varies linearly with frequency. This is equivalent to a constant time delay to the signal within the passband, and thus, preserves the original waveform [17]. The cut-off frequency can be programed on-the-fly from 15Hz to a few hundred hertz. In order to improve signal-to-noise ratio, the accelerometer signal is finally amplified by a programmable amplifier. The overall amplification gain can be set from ×1.9 to ×190. A distinct feature of the integrated accelerometer wing is that the cutoff frequencies and gains are remotely programmable. This feature is achieved by adopting digital potentiometers (Digipots), whose resistance value can be programed on-the-fly through an I^2C interface from the Martlet microcontroller. The programmable cutoff frequencies and gains offer great convenience in field testing. When a new set of cutoff frequencies and gains is needed, a wireless command

(a) Integrated accelerometer wing (2.0 in × 2.25 in)

(b) Weatherproof package (2.28in × 2.52in × 1.38in)

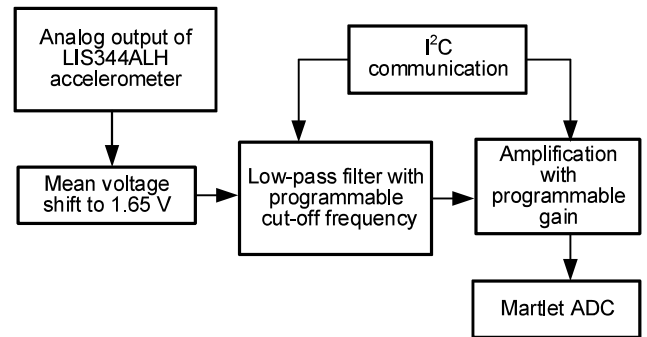Fig. 2. Integrated accelerometer wing with weatherproof package

Fig. 3. Functional diagram of integrated accelerometer wing

from the server can easily achieve immediate setting update for all Martlet nodes.

The integrated accelerometer wing is placed into a compact weatherproof enclosure with a dimension of 2.28in (L) × 2.52in

(W) × 1.38in (H), for firm installation of the accelerometer onto a structural surface (Fig. 2(b)). As a result, the integrated accelerometer wing is connected to the Martlet node with an eight-wire cable. Three wires in the cable are allocated for the acceleration output signals (X, Y and Z channels), two for I^{2}C
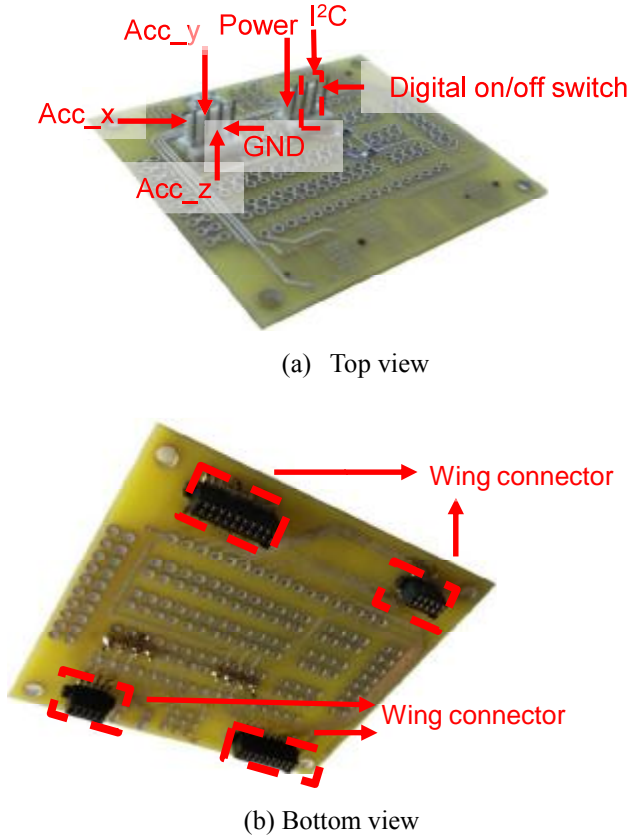

(a) Top view

(b) Bottom view

Fig. 4. Interface wing between Martlet node and integrated accelerometer wing (2.5 in × 2.25 in)
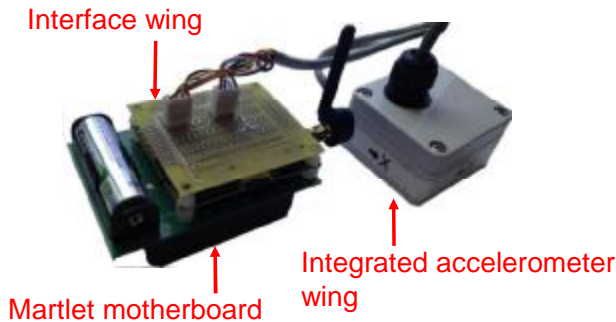
Fig. 5. Integrated accelerometer wing with Martlet node

communication, one for power, one for ground, and the last one for a digital signal that allows the Martlet motherboard to power the accelerometer wing on and off. An interface wing is developed to allow the integrated accelerometer wing to work with Martlet motherboard (Fig. 4). Two Molex headers are soldered on the interface wing for the eight-wire cable to connect to the Martlet motherboard (Fig. 4(a)). Four wing connectors are soldered at the bottom of the interface wing (Fig. 4(b)), so that the wing can stack atop and plug onto the motherboard. Fig. 5 shows a set of integrated accelerometer wing stacked atop a Martlet motherboard. The current consumption of the tri-axial integrated accelerometer wing is ~12 mA (referenced at 3.3V) under normal working conditions and ~1 μA when powered off into sleep mode.

## VALIDATION OF THE WIRELESS ACCELERATION MEASUREMENT

In order to evaluate the performance of the Martlet wireless node and the integrated accelerometer wings, laboratory experiments are conducted. One Martlet node with an integrated accelerometer wing is installed at each floor of a four-story aluminum structure (#1~#4 in Fig. 6(a)). Another Martlet node (#0) is installed at base. The four-story structure is mounted on a shake table which applies base excitation to the structure. Although the Martlet accelerometer wing is capable of capturing tri-axial accelerations, only one axis is needed in this experiment. A high-precision cabled accelerometer is also installed on the base (#0) and the first floor (#1) as reference. The acceleration measurements from the integrated accelerometer wings are first compared with those of high-precision cabled accelerometers. Modal properties of the four-story structure are then extracted from the wireless acceleration data. Finally, finite element (FE) model updating of the four-story structure is performed using the extracted modal parameters.

## Description of the four-story structure and experimental setup

The entire structure is made of aluminum, including rigid plates as floors and flexible strips as columns. The properties of the frame structure are shown in Table I. Fig. 6(b) shows the close-up view of the base plate and the first floor. At the base and the first floor, a Martlet node with an integrated accelerometer and a high-precision cabled accelerometer (Silicon Designs 2012-002) are installed side by side. At other

Table I. Properties of the four-story structure

	Parameter	Value
Aluminum plate	Weight (lb)	11.310
Aluminum column	Length (in)	12
	Width (in)	1
	Thickness (in)	0.125
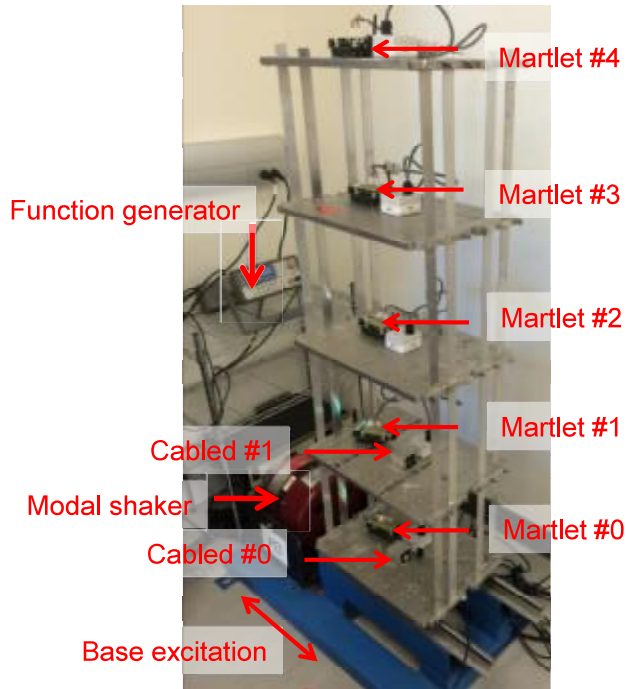
(a) Photo of complete experimental setup
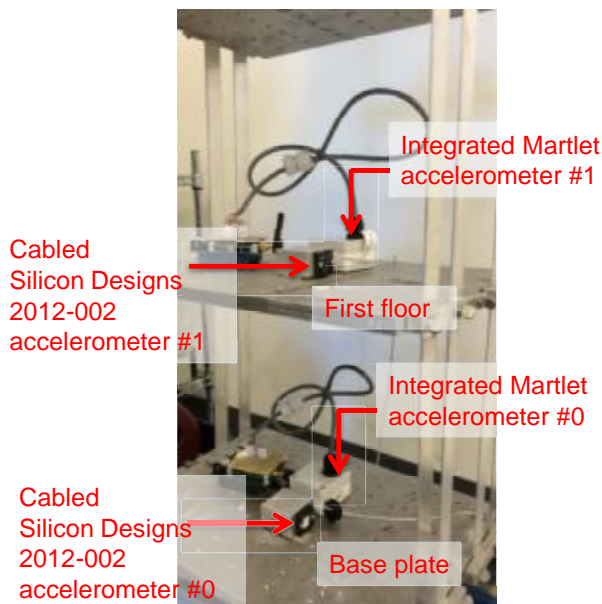
(b) Close-up view of experimental setup

Fig. 6. Experimental setup for the integrated accelerometer wing

higher floors, only a Martlet node with an integrated accelerometer is installed (Fig. 6(a)). The weight of a Martlet node with an integrated accelerometer is 0.75 lb, and the weight

of the cabled accelerometer on a mounting block is 0.375lb. Both weights are trivial for actual civil structures, but cannot be neglected on this laboratory structure. Because the modal shaker only generates single-direction ground excitation, only the x-axis of the integrated accelerometer wing is used to collect horizontal floor acceleration. In the following experiments, the amplification gain of the integrated accelerometer wings is set to ×20, and the cutoff frequency is set as 25Hz. The sampling frequency of the wireless sensing system is set as 1,000Hz. The cabled accelerometer data is sampled by a commercial National Instruments data acquisition system. A signal conditioner is connected between the accelerometer and cabled data acquisition system, the gain and cutoff frequency of which is set to be same as the integrated accelerometer wing. The sampling frequency of the cabled sensing system is set as 1,652Hz.

Comparison between wireless and cabled sensing systems

Fig. 7 compares the time history data from the cabled accelerometers and the integrated accelerometer wings. The acceleration data were collected when the modal shaker generates the record of 1940 El Centro NS earthquake excitation to the structure. Fig. 7(a) and 7(b) compare the wireless and cabled measurements on the base, and Fig. 7(c) and 7(d) shows the comparison on the first floor. Comparisons are shown for a total period of 10 seconds, and for a close-up view of 3 seconds. All figures illustrate excellent agreement between the data sets collected by the wireless and cabled systems. It is demonstrated that the integrated accelerometer wing is capable of providing high-quality acceleration measurements that are comparable with a high-precision cabled system in this experiment.

Modal analysis results using wireless sensor data

In order to obtain acceleration data for extracting modal properties, a chirp signal (increasing from 0Hz to 15Hz in 15s) is generated as ground excitation. During the modal test, the cabled reference accelerometers are removed from the structure; only the wireless system remains on the structure. Fig. 8 presents two sets of example acceleration data recorded by the Martlet nodes installed on the first and second floors, as well as the corresponding frequency spectra. Similar peak resonance frequencies can be observed between the two spectra.

The eigensystem realization algorithm (ERA) [5] is applied to the impulse response functions obtained from wireless sensing data with chirp ground excitation. Modal properties of the four-story structure are extracted. Fig. 9 shows the first four mode shapes and resonance frequencies. The extracted frequencies match with the peaks in the example frequency spectra (Fig. 8). The mode shapes also agree with the expectation for a shear building structure.
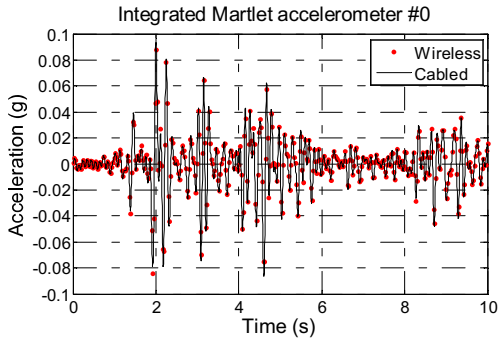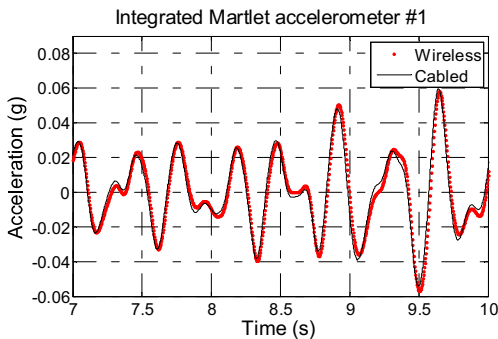
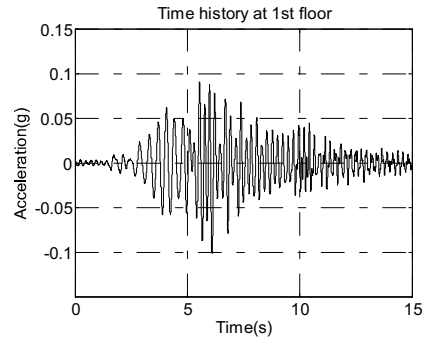(a) Comparison for integrated Martlet accelerometer #0
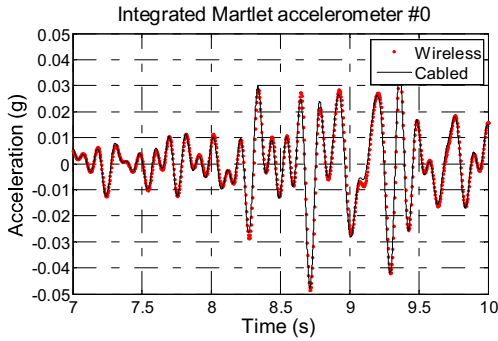
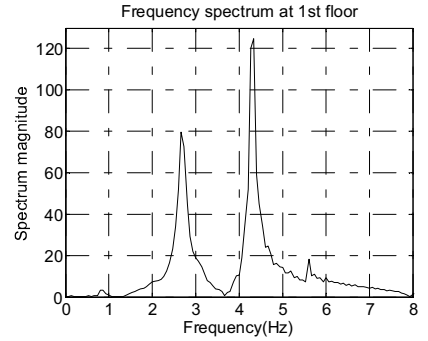(b) Close-up comparison for integrated Martlet accelerometer #0
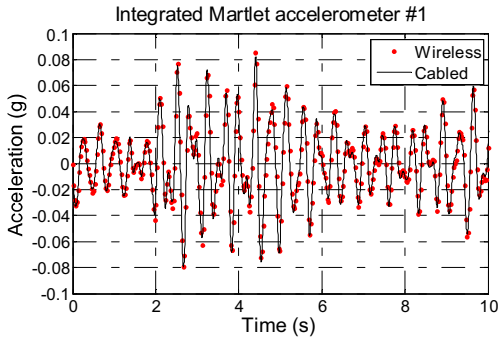
(c) Comparison for integrated Martlet accelerometer #1

(d) Close-up comparison for integrated Martlet accelerometer #1

Fig. 7. Comparison between integrated Martlet accelerometer wing and cabled accelerometer
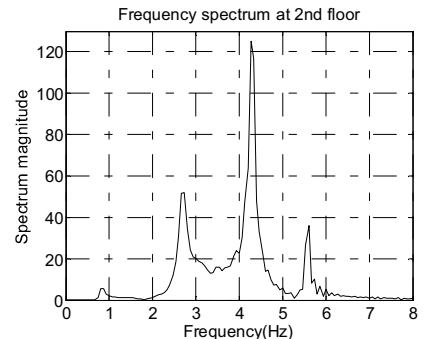

(a) Time history of first floor response

(b) Frequency spectrum of first floor response
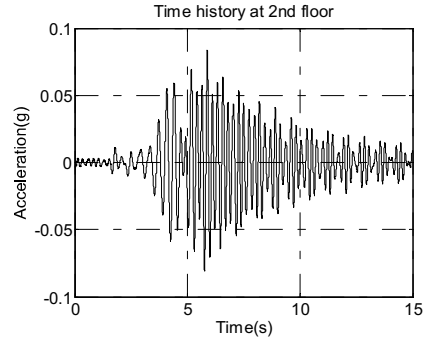
(c) Time history of second floor response

(d) Frequency spectrum of second floor response

Fig. 8. Example response records and corresponding frequency spectra records
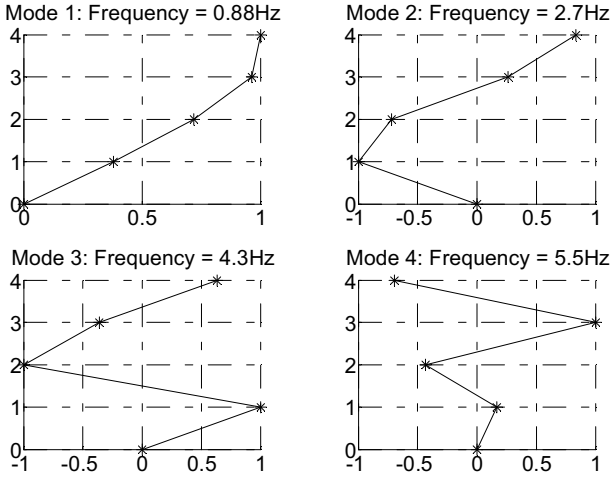
Fig. 9. First four mode shapes of the four-story structure obtained from the wireless sensors with chirp excitation

Finite element model updating

With rigid plates as floors, the four-story shear frame structure can be simplified as a lumped-mass model with four degrees of freedom (DOFs) (Fig. 10). The nominal parameter values of the simplified model are listed in Table II. Since the
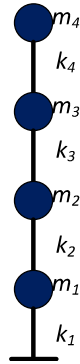

Fig. 10. Simplified four-story structure model

Table II. Floor mass and nominal inter-story stiffness values

	Parameter	Value
Mass (lb)	m_1	12.060
	m_2	12.060
	m_3	12.060
	m_4	12.060
Stiffness (kips·in)	k_1	0.01
	k_2	0.01
	k_3	0.01
	k_4	0.01

cabled sensors are removed from the structure during the modal test, the mass of each floor only includes the contributions from aluminum plate as well as the wireless sensors. The weight of the columns is neglected. Overall inter-story stiffness of each floor is contributed by the fixed-end shear stiffness of the aluminum columns.

During the FE model updating process, only the four stiffness values are selected as updating parameters. The mass values are considered to be accurate. For the four-story structure, the stiffness can be updated as

$$\mathbf{K} = \mathbf{K}_0 + \sum_{i=1}^{4} \alpha_i \mathbf{K}_{0,i} \qquad (1)$$

where $\mathbf{K}_0$ is the initial stiffness matrix assembled using nominal stiffness values prior to model updating; α_i is the stiffness parameter to be updated; $\mathbf{K}_{0,i}$ are constant sensitivity matrices that represent contributions corresponding each inter-story stiffness [18, 19]. In this study, a modal dynamic residual approach and a modal property difference approach are utilized to perform the FE model updating [20, 21].

The modal dynamic residual approach adopts a convex formulation by minimizing following residual:

$$\text{minimize} \qquad \sum_{i=1}^{4} \left\| \left(\mathbf{K} - \omega_i^2 \mathbf{M} \right) \boldsymbol{\psi}_i \right\|^2 \qquad (2a)$$

$$\text{subject to} \qquad \boldsymbol{\alpha}_L \leq \boldsymbol{\alpha} \leq \boldsymbol{\alpha}_U \qquad (2b)$$

where $\|\cdot\|$ denotes the 2-norm of a vector; $\boldsymbol{\alpha}_L$ denotes the element-wise lower bound for vector $\boldsymbol{\alpha}$; $\boldsymbol{\alpha}_U$ denotes the element-wise upper bound for vector $\boldsymbol{\alpha}$; ω_i and $\boldsymbol{\psi}_i$ represent the i-th frequency and mode shape, previously extracted from experimental data.

The modal property difference approach aims to minimize the difference between experimental and analytical natural frequencies, as well as the difference between experimental and analytical mode shapes of the structure.

$$\text{minimize} \quad \sum_{i=1}^{4} \left(\frac{\omega_{\text{FE},i} - \omega_i}{\omega_i} \right)^2 + \sum_{i=1}^{4} \left(\frac{1 - \sqrt{\text{MAC}_i}}{\sqrt{\text{MAC}_i}} \right)^2 \qquad (3a)$$

$$\text{subject to} \qquad \boldsymbol{\alpha}_L \leq \boldsymbol{\alpha} \leq \boldsymbol{\alpha}_U \qquad (3b)$$

where $\omega_{\text{FE},i}$ and ω_i represent the analytical (from FE model) and experimentally extracted natural frequencies, respectively; MAC_i represents the modal assurance criterion evaluating the difference between the i-th analytical and experimentally extracted mode shapes. A nonlinear least square optimization solver, 'lsqnonlin' in MATLAB toolbox [22], is adopted to numerically solve both model updating approaches. Table III summarizes the model updating results of the modal dynamic residual approach and modal property difference approach. The model updating results from two approaches are close to each

Table III. Updated stiffness values (kips·in)

Updating parameter	Modal dynamic residual approach	Modal property difference approach
k_1	0.0070	0.0072
k_2	0.0081	0.0081
k_3	0.0091	0.0090
k_4	0.0147	0.0147

other. The largest difference occurs with k_1. Both sets of the optimal stiffness values are different from the initial estimations.

Table IV compares the modal properties obtained from experimental results and three FE models, i.e. the initial model and two updated models. Using parameters of each FE model, the objective functions in Eq. (2) and (3) are evaluated and the values are also listed in Table IV. The natural frequencies of the updated FE model from modal dynamic residual approach are close to the experimental results, with the largest error being 0.70%. The modal property difference approach gives higher accuracy in all four natural frequencies. In terms of mode shapes, the modal dynamic residual approach demonstrates similar performance to the modal property difference approach. Nevertheless, both approaches generate modal properties that are much closer to experimental results than the initial model. Finally, the achieved values of the objective functions for both approaches decrease significantly from the values of the initial model. As intended, the modal dynamic residual approach minimizes the objective function in Eq. (2); the modal property difference approach minimizes the objective function in Eq.(3).

SUMMARY AND DISCUSSION

This paper presents the latest development and validation of Martlet, a next-generation, low-cost wireless sensing system for structural health monitoring. The Martlet node provides an extensible wireless platform which is able to execute high-frequency data acquisition and high-speed onboard computation. Standardized wing boards can be easily plugged in with the Martlet motherboard, which allows simultaneous data acquisition from multiple sensors of various types. The onboard Micro SD card significantly extends the data storage space of the Martlet node.

The newly developed low-cost integrated accelerometer wing can provide accurate acceleration measurement for dynamic testing. The amplification gain and cutoff frequency of the integrated accelerometer wings can be conveniently changed on the fly. In the laboratory experiment, the accuracy of the integrated accelerometer wing is validated with high-precision cabled accelerometers. Furthermore, modal analysis is successfully conducted using the wireless data. It is shown the wireless sensing system is capable of providing consistent and reliable resonance frequencies and mode shapes. Finally, an FE model is updated based upon the modal properties extracted from the wireless data. Both modal dynamic residual approach and modal property difference approach are utilized to perform the FE model updating, and the stiffness parameters converge to similar optimal values. The updated FE models from both model updating approaches provide similar modal properties as the experimental results.

Future research will continue to improve the Martlet system in terms of power efficiency, reliability, and usability. In the meantime, the performance of the integrated accelerometer wing will be evaluated through field experiments.

Table IV. Comparison of modal updating results between modal dynamic residual approach and modal property difference approach

	Experimental results	Initial FE model			Modal dynamic residual approach			Modal property difference approach		
	f_n (Hz)	f_n (Hz)	Δf_n (%)	MAC	f_n (Hz)	Δf_n (%)	MAC	f_n (Hz)	Δf_n (%)	MAC
1st mode	0.88	0.99	12.02	0.99	0.88	0.70	1.00	0.88	0.01	1.00
2nd mode	2.75	2.85	3.64	0.95	2.74	0.44	0.99	2.75	0.02	1.00
3rd mode	4.30	4.36	1.47	0.74	4.29	0.13	1.00	4.30	0.01	1.00
4th mode	5.53	5.35	3.21	0.70	5.53	0.04	0.99	5.53	0.03	1.00
Objective in Eq.(2)		1.273×10^{-4}			1.038×10^{-5}			1.058×10^{-5}		
Objective in Eq.(3)		4.400×10^{-2}			8.899×10^{-5}			1.832×10^{-5}		

REFERENCES

[1]FHWA, "*National Bridge Inventory*," U.S. Department of Transportation, Federal Highway Administration, Washington, D.C.2013.

[2]ASCE, *Report Card for America's Infrastructure*. Reston, VA: American Society of Civil Engineers, 2013.

[3]J. M. Ko and Y. Q. Ni, "Technology developments in structural health monitoring of large-scale bridges," *Engineering Structures,* vol. 27, pp. 1715-1725, 2005.

[4]C. R. Farrar, H. Sohn, F. M. Hemez, M. C. Anderson, M. T. Bement, P. J. Cornwell*, et al.*, "*Damage Prognosis: Current Status and Future Needs*," Los Alamos National Laboratory, Los Alamos, NM Report No. LA-14051-MS, 2003.

[5]J. N. Juang and R. S. Pappa, "An eigensystem realization algorithm for modal parameter identification and modal reduction," *Journal of Guidance Control and Dynamics,* vol. 8, pp. 620-627, 1985.

[6]B. Peeters and C. E. Ventura, "Comparative study of modal analysis techniques for bridge dynamic characteristics," *Mechanical Systems and Signal Processing,* vol. 17, pp. 965-988, 2003.

[7]Z. C. Yang, Z. F. Yu, and H. Sun, "On the cross correlation function amplitude vector and its application to structural damage detection," *Mechanical Systems and Signal Processing,* vol. 21, pp. 2918-2932, 2007.

[8]X. Yi, D. Zhu, Y. Wang, J. Guo, and K.-M. Lee, "Transmissibility-function-based structural damage detection with tetherless mobile sensors," *Proceeding of the Fifth International Conference on Bridge Maintenance, Safety and Management*, Philadelphia, PA, USA, 2010.

[9]M. Çelebi, "*Seismic Instrumentation of Buildings (with Emphasis on Federal Buildings)*," United States Geological Survey, Menlo Park, CA Report No. 0-7460-68170, 2002.

[10]J. P. Lynch and K. J. Loh, "A summary review of wireless sensors and sensor networks for structural health monitoring," *The Shock and Vibration Digest,* vol. 38, pp. 91-128, 2006.

[11]R. A. Swartz, D. Jung, J. P. Lynch, Y. Wang, D. Shi, and M. P. Flynn, "Design of a wireless sensor for scalable distributed in-network computation in a structural health monitoring system," in *Proceedings of the 5th International Workshop on Structural Health Monitoring*, Stanford, CA, 2005

[12]Y. Wang, J. P. Lynch, and K. H. Law, "A wireless structural health monitoring system with multithreaded sensing devices: design and validation," *Structure and Infrastructure Engineering,* vol. 3, pp. 103-120, 2007.

[13]T. Nagayama and B. F. Spencer, Jr., "*Structural health monitoring using smart sensors*," Newmark Structural Engineering Laboratory, University of Illinois at Urbana-Champaign, Urbana, IL Report No. NSEL-001, 2007.

[14]M. Kane, D. Zhu, M. Hirose, X. Dong, B. Winter, M. Häckell*, et al.*, "Development of an extensible dual-core wireless sensing node for cyber-physical systems " in *Proceedings of SPIE, Sensors and Smart Structures Technologies for Civil, Mechanical, and Aerospace Systems*, San Diego, CA, USA, 2014

[15]T. Cooklev, *Wireless Communication Standards : a Study of IEEE 802.11, 802.15, and 802.16*. New York: Standards Information Network IEEE Press, 2004.

[16]X. Dong, S. Chen, D. Zhu, M. Kane, Y. Wang, and J. P. Lynch, "High-speed heterogeneous data acquisition using Martlet - a next-generation wireless sensing node," in *Proceeding of the 6th World Conference on Structural Control and Monitoring*, Barcelona, Spain, 2014

[17]P. Horowitz and W. Hill, *The Art of Electronics*, 2nd ed. Cambridge, England: Cambridge University Press, 1989.

[18]D. Zhu and Y. Wang, "Substructure model updating through iterative convex optimization," in *Proceeding of the ASME 2012 Conference on Smart Materials, Adaptive Structures and Intelligent Systems (SMASIS 2012)*, Stone Mountain, GA, 2012

[19]D. Zhu and Y. Wang, "Substructure model updating through iterative convex optimization," in *Proceedings of the ASME 2012 Conference on Smart Materials, Adaptive Structures and Intelligent Systems*, Stone Moutain, GA, 2012

[20]D. Zhu, X. Dong, and Y. Wang, "An iterative convex optimization procedure for structural system identification," in *Proceedings of 2013 ASCE International Workshop on Computing in Civil Engineering*, Los Angeles, CA, 2013

[21]B. Jaishi and W. X. Ren, "Damage detection by finite element model updating using modal flexibility residual," *Journal of Sound and Vibration,* vol. 290, pp. 369-387, 2006.

[22]MathWorks Inc., *Control System Toolbox : for Uses with MATLAB® : Getting Started*, Version 6. ed. Natick, MA: MathWorks Inc., 2005.